JOIV : Int. J. Inform. Visualization, 8(3) - September 2024 1118-1125

INTERNATIONAL JOURNAL ON INFORMATICS VISUALIZATION

journal homepage : www.joiv.org/index.php/joiv

Multi-spatial Resolution Imagery to Estimate Above-Ground Carbon Stocks in Mangrove Forests

Eva Purnamasari [a,*], Muhammad Kamal [b], Pramaditya Wicaksono [b], Muhammad Faqih Hidayatullah [c], Bigharta Bekti Susetyo [d]

[a] *Vocational School in Remote Sensing and Geographic Information System, Universitas Negeri Padang, Padang, Indonesia*
[b] *Geographic Information Science, Universitas Gadjah Mada, Jalan Bulaksumur, Sleman, Indonesia*
[c] *Korea-Indonesia Marine Technology Cooperation Research Center, Jalan MH. Thamrin, Jakarta, Indonesia*
[d] *Department of Geography, Universitas Negeri Padang, Jalan Prof. Dr. Hamka, Padang, Indonesia*
Corresponding author: [*]evapurnamasari@fis.unp.ac.id

***Abstract*— Mangroves are a type of vegetation that can absorb carbon and have an essential role in controlling CO_2 levels in the atmosphere. Mangroves can absorb carbon better than terrestrial ecosystems because of their ability to bury carbon in sediment. This research aims to compare and measure the carbon stock content above the surface of mangroves in the field using multi-spatial resolution imagery, namely, Landsat 8 OLI, Sentinel 2A, and Planetscope. Field carbon calculations were carried out using the allometric method based on mangrove species. The calculation results are then linked through regression analysis with the vegetation index Difference Vegetation Index (DVI) results. The total carbon obtained from PlanetScope imagery was 535.27 tons, Sentinel 2A imagery was 549.23 tons, and Landsat 8 OLI imagery was 533.57 tons. Among the three images used, based on Sentinel 2A statistical analysis reflects the possibility of overfitting or the best with higher r and R^2 values in the calculations. However, based on SE accuracy tests, PlanetScope has better accuracy than the other two images. Apart from that, the accuracy test results using a 1:1 goodness of fit plot for each image, the distribution pattern of mangrove carbon stock estimates shows that the entire model in mapping mangrove carbon stocks is over-estimated. The overestimated results are possible because more objects around the mangrove, especially canopy density, are recorded by remote sensing sensors compared to tree diameter as input for field carbon results.**

***Keywords*—Multi-resolution spatial imagery; carbon stock; mangroves.**

Manuscript received 9 Oct. 2023; revised 13 Jul. 2024; accepted 2 Aug. 2024. Date of publication 30 Sep. 2024.

I. INTRODUCTION

Vegetation plays a vital role in absorbing carbon in the atmosphere. Apart from that, vegetation also plays a crucial role in maintaining global climate stability [1]. Apart from the terrestrial role of forests as carbon sinks, new evidence shows that carbon can be stored in the biomass and sediment of vegetation in tidal swamp ecosystems such as mangroves and seagrass beds [2]. This coastal vegetation carbon stock is called blue carbon [3]. Carbon stocks stored in vegetation, especially trees, are essential for environmental harmony from excessive emissions because trees and other photo-autotrophic organisms undergo photosynthesis during the day. This process requires an essential component of CO_2 from the atmosphere. Carbon Stock Mapping availability is critical for supporting land use planning, such as understanding the consequences of replacing mangrove ecosystems and their ecological services [4], [5].

Mangroves are a type of vegetation that can absorb carbon and have an essential role in controlling CO_2 levels in the atmosphere. Mangroves can absorb carbon better than terrestrial ecosystems because of their ability to bury carbon in sediment. As an ecosystem, mangroves are a place for various types of biotas to live. Besides that, mangrove forests function as providers of environmental services because they are the most effective blue carbon sinks. Mangrove forests are one of the most diverse ecosystems on Earth and deliver numerous provisioning, regulating, cultural, and supporting services that benefit coastal and inland communities [6]–[8]. Damaged mangrove forests will affect the ability of mangrove forests to absorb carbon. The existence of mangroves must continue to be preserved and improved, as well as both the quality and

quantity of the forest so that they function well in reducing global warming. The conversion of mangrove forests for aquaculture, tourism, and agricultural purposes has disrupted ecosystem stability and reduced physical and biological mangrove functions, affecting the existence of vulnerable mangrove species that are rare or limited [9]. Previous studies have shown that mangrove conversion to shrimp ponds generates substantial losses of biomass and soil carbon stocks [10]–[13]. This research used multi-spatial resolution images, including Landsat 8 OLI, Sentinel 2A, and Planetscope, each of which has a different spatial resolution, namely 30 m, 10 m, and 3 m. According to Planet Labs' data about product specifications, the advantages of PlanetScope's imagery are having a speedy iteration time (i.e., for 1 day), carrying four spectral bands (blue, green, red, and near-infrared), and high spatial resolution (3 m). A fast temporal resolution is expected to be able to describe the information in actual relation between the imagery recording date and in-situ measurements [14]. The varying characteristics of multispectral satellite images and incredibly different image spatial resolution sizes will produce different levels of information detail. This research aims to assess the ability of several images with different spatial resolutions to estimate above-surface carbon stocks in the Bedul Mangrove Area, Banyuwangi. Carbon stocks are closely related to biomass. Biomass can be highlighted from spectral transformations related to vegetation, often known as the vegetation index. While spectral bands are commonly used in remote sensing-based AGB estimation, studies have shown that the inclusion of vegetation indices and texture variables can significantly improve results, particularly in dense tropical forests [15], [16]. The vegetation index is a form of spectral transformation of multispectral images to highlight aspects of vegetation density or things related to vegetation density, such as biomass.

II. Materials and Method

A. Research Site

This research will be carried out in the Blok Bedul Mangrove Forest area. This forest area is included in the Alas Purwo National Park area in Bloksolo Hamlet, Sumberasri Village, Purwoharjo District, Banyuwangi Regency. The Alas Purwo National Park area, based on the minutes of measurement dated 27 May 1983, has an area of 43,420 ha. The lowland tropical rainforest ecosystem is the primary ecosystem type in the Alas Purwo National Park area. In contrast, the mangrove forest in the Alas Purwo National Park area has an area of 1,200 ha.

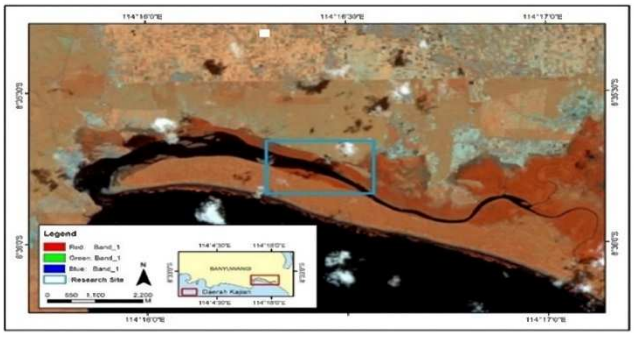

Fig. 1 Research site

B. Image Dataset

Landsat 8 OLI in this study carried out radiometric corrections for converting Digital Number (DN) values to Top of Atmosphere (TOA) solar angle reflectance. Apart from that, atmospheric correction was also carried out using Dark Object Subtraction (DOS). The Landsat 8 OLI image is radiometrically calibrated, geometrically co-registered, and orthorectified [17]. This DOS was chosen because the field data parameters for image correction were unknown. Also, no known atmospheric effects model could assume the atmospheric conditions when the image data was recorded.

In this study, sentinel 2A carried out atmospheric correction using the DOS method because the Sentinel 2A image has been radiometrically corrected in the form of TOA reflectance. So, the following correction process is an atmospheric correction.

Planetscope images are available in images corrected to Surface Reflectance and have undergone previous radiometric correction. Apart from that, geometric correction was not carried out in this research because the Planetscope image used had undergone a geometric correction process, so this Planetscope image was not subjected to radiometric correction or geometric correction.

The vegetation index is an optical measurement of the greenness of the vegetation canopy, the composite nature of leaf chlorophyll, leaf area, structure, and vegetation canopy cover. The aim of using this vegetation index is to determine the level of accuracy of estimates and determine an accurate vegetation index in calculating the AGB of mangrove forests [18]. The vegetation index used in this research is DVI (Difference Vegetation Index). The relationship between field carbon values and DVI index values is vital. DVI has the highest AGC estimation accuracy as compared to EVI and NDVI [19].

C. Field Sampling

Sampling uses several plots. The plots are square, and the plot size to be used is 20 x 20 m divided into three parts, namely 20 x 20 m, 10 x 10 m, and 5 x 5 m, adjusted to the spatial resolution of each image used. Each plot size is used to measure different tree diameters. A plot measuring 20 x 20 m is used to measure trees with a diameter > 20 cm, a plot measuring 10 x 10 m is used to measure trees with a diameter of 10 – 20 cm, and a plot measuring 5 x 5 m is used for measure trees < 10 cm in diameter (SNI 7724:2011) [20].

D. AGC Estimation and Mapping

The biomass calculated in this research is the biomass above the ground surface. Mangrove biomass was calculated using the allometric method based on the mangrove species in the Bedul Mangrove Area, Banyuwangi. This research uses allometric equations which refer to the allometric equations of Komiyama [21], because this equation is used for Asian mangroves. The allometric equations produced the AGB value rather than directly creating the AGC value [22]. Above-surface carbon stock values are obtained from the above-surface biomass value approach. The rules used are based on SNI 7724:2011, calculating carbon from biomass.

The normality test tests data to see whether the residual values are normally distributed. Normally distributed data will reduce the possibility of bias. In this study, to determine

the normality of data distribution using the Kolmogorov-Smirnov Test, the Dn value must not exceed the Kolmogorov-Smirnov table value limit. Correlation analysis is used to find the degree of relationship between variables. The correlation coefficient is the measure used to determine the degree of relationship.

The results of carbon stock estimation in the field are then seen in relation to inputs that can pass the significance limit of the correlation test. The amount of carbon stock is usually represented in units of tons/ha. Regression analysis was carried out to build an equation for biomass content using fieldwork data as the dependent variable (Y) with input that could pass the significance limit of the correlation test as the dependent variable (X). The regression results with the highest correlation will be transformed to produce a carbon estimation map.

Analyzing the comparative results of estimates of above-ground carbon stocks in mangrove forests using multi-spatial resolution imagery requires accuracy tests. The accuracy test uses the Standard Error of Estimate (SEE) method, which in its formula uses the carbon value calculated in the field with the carbon value resulting from the regression equation from the input, which can pass the significance limit of the correlation test used on different types of images. The better the level of accuracy is indicated by the lower the value obtained from the standard error of the estimate. The formula equation for the accuracy test in this research is as follows:

$$SEE = \sqrt{\frac{\sum(y-y')^2}{n-2}} \quad (1)$$

Information:

y' = predicted carbon value in the field (tons/ha)

y = carbon value in the field (tons/ha)

n = number of samples

Apart from SEE, the accuracy test for estimating carbon stocks above the mangrove surface was carried out using a 1:1 goodness of fit plot. The function of this accuracy method is to try to see whether the estimated data pattern and whether the accuracy test sample has an overestimated or underestimated pattern by looking at the slant of the linear line of the sample plot, which is bounded by the red line as the ideal value of 1:1 between the field value and the estimate[23]. If the distribution of the linear plot is biased toward the image estimation data, then overestimation occurs, and underestimation occurs when the linear plot is biased toward field data.

III. Result and Discussion

A. Field Data and Carbon Stocks

Field data collected during fieldwork includes mangrove species, tree DBH, tree height, hemisphere photos to determine canopy density, and photos of the situation around the sample point. Tree height data and hemisphere photos are additional data used if needed when using the allometry formula. Technical fieldwork at each sample point begins with stretching a rope 20x20 meters long. After that, the mangrove species in the sample plot will be identified. A size of 20x20 meters is used to collect data on mangrove tree categories. The size of 10x10 meters is used to collect data on pole-category mangroves. The length of 5x5 meters is used to collect data on the mangrove sapling category. In the category of each sample point, DBH and tree height are measured, which are then filled in in the field worktable provided.

Based on the identification results carried out by Alas Purwo National Park researchers, 27 true mangroves were found. Of the 27 species, 24 types around the Segara Anak River are dominated by *Rhizophora mucronata*, *Ceriops tagal*, and *Bruguiera gymnorhiza*. The results of the research that was carried out show that 14 species of mangroves were found around the Segara Anak River. The measurement results based on the parameters used in this research show different results at each observation location point. The parameters used include average tree diameter, tree height, canopy cover, and dominant species at each observation sample point.

TABLE I
FIELD DATA

Point Number	Coordinate		Average tree diameter (cm)	Average tree height (m)	Fcover	Dominant Species
	X	Y				
1	-8.596	114.257	27.75	10.85	0.40	*R. Mucronata*
2	-8.595	114.267	29.27	11.74	0.34	*E. Agallocha*
3	-8.598	114.273	40.93	14.59	0.33	*R. Mucronata*
4	-8.598	114.273	54.77	23.06	0.14	*R. Mucronata*
5	-8.597	114.273	39.18	17.64	0.18	*R. Mucronata*
6	-8.599	114.277	45.00	13.68	0.22	*A. Officinalis*
7	-8.599	114.277	40.88	18.98	0.21	*R. Apiculata*
8	-8.600	114.277	50.58	18.85	0.09	*R. Apiculata*
9	-8.600	114.280	47.85	11.91	0.05	*R. Apiculata*
10	-8.601	114.279	47.05	23.36	0.21	*R. Apiculata*
11	-8.592	114.270	38.46	15.96	0.31	*R. Mucronata*
12	-8.592	114.270	28.17	8.21	0.18	*C. Decandra*
13	-8.592	114.268	36.31	14.13	0.29	*S. Alba*
14	-8.590	114.265	22.57	5.72	0.09	*C. Tagal*
15	-8.598	114.282	48.83	19.54	0.20	*R. Apiculata*
16	-8.597	114.282	48.20	16.73	0.17	*R. Apiculata*
17	-8.597	114.278	41.30	19.06	0.15	*S. Alba*
18	-8.595	114.276	34.23	16.12	0.27	*S. Alba*
19	-8.593	114.272	35.34	10.83	0.15	*S. Alba*
20	-8.592	114.273	22.78	5.96	0.18	*C. Decandra*

This research obtained information about mangrove biomass content using the allometric method. The allometric formula used is not separated into formulas for leaves, twigs, and stems like in previous studies. However, it uses an allometric formula based on mangrove species. The allometric formula used is quite diverse because 14 mangrove species have been obtained during fieldwork. The mangrove canopy is also not counted in biomass and carbon calculations because the allometry method only uses data on tree diameter at breast height (DBH).

Mangrove biomass can be calculated using variables such as tree diameter and height data. In this research, the calculation of mangrove tree biomass data was not carried out destructively but using a tree diameter at breast height (DBH) data approach, which was then entered into the allometric equation. The largest carbon storage on land is generally found in the tree component. Different soil conditions between sites might impact this carbon stock discrepancy [24].

TABLE II
BIOMASS AND CARBON STOCK

No Titik	Biomass (ton/ha)	Carbon (ton/ha)	Dominant Species
1	193.53	90.96	*R. Mucronata*
2	114.18	53.66	*E. Agallocha*
3	210.71	99.03	*R. Mucronata*
4	242.75	114.09	*R. Mucronata*
5	121.23	56.98	*R. Mucronata*
6	123.41	58.00	*A. Officinalis*
7	109.09	51.27	*R. Apiculata*
8	133.77	62.87	*R. Apiculata*
9	113.95	53.56	*R. Apiculata*
10	137.76	64.75	*R. Apiculata*
11	108.16	50.84	*R. Mucronata*
12	45.35	21.32	*C. Decandra*
13	63.94	30.05	*S. Alba*
14	27.36	12.86	*C. Tagal*
15	234.01	109.98	*R. Apiculata*
16	154.00	72.38	*R. Apiculata*
17	69.58	32.70	*S. Alba*
18	53.01	24.92	*S. Alba*
19	70.73	33.24	*S. Alba*
20	38.10	17.91	*C. Decandra*

B. AGC Estimation and Mapping

To minimize any suspicion from the processing results, a normality test was carried out to determine the appropriateness of the data used in further analysis, namely correlation and regression. The requirement for parametric statistical analysis, namely regression, is that the data must be normally distributed. Table III shows the result of the normality test processing. The input data used is 20 data based on the number of samples that have been obtained. Normal or abnormal data can be determined from the values in the Dn and KS Tables. If the Dn value is more than the KS Table, namely 0.30, the data is considered abnormal, conversely, if the Dn value is less than 0.30, the data is considered normal, and further statistical analysis can be carried out. Based on these results, all input data produces Dn < KS Table values so that the 20 data used for further analysis have fulfilled the assumptions in parametric statistics-based research. From the results of the normality test processing, it can be concluded that the data that has been obtained is suitable for use in statistical analysis.

TABLE III
NORMALITY TEST

Image	Input	Statistic				
		Sample	Mean	StDev	Dn	KS Table
	Carbon Observed	20	55.37	29.94	0.13	0.30
Planetscope	DVI	20	0.18	0.03	0.10	0.30
Sentinel 2A	DVI	20	0.17	0.04	0.16	0.30
Landsat 8 OLI	DVI	20	0.20	0.03	0.10	0.30

The correlation test is a statistical analysis technique used to find the relationship between two quantitative variables. This research examines the relationship between carbon values in the field and the vegetation index values used. The correlation coefficient (r) is a variable that can show the closeness of the relationship between two or more variables concerning the dependent variable. The significance level used in this research is 95% using the Pearson Product Moment correlation method. Correlation analysis was carried out to determine the relationship between vegetation index values and field carbon values. Input values that can pass the significance limit of the r value for the number of samples (n) and have a significant relationship with field carbon are used as input in empirical modeling through regression analysis.

TABLE IV
CORRELATION TEST

Image	Input	Normality Data	R
Planetscope	DVI	Normal	0.82
Sentinel 2A	DVI	Normal	0.85
Landsat 8 OLI	DVI	Normal	0.70

The regression results from the three multi-resolution images used by the Sentinel 2A image had the highest regression value of 0.7244, which means that as much as 72.44% of the variation in field carbon values can be explained by pixel values from the DVI transformation. The equation that shows the relationship between the DVI index and carbon value is $y = 1641.8x - 241.46$. The Planetscope image has a regression value of 0.6732 with the equation $y = 1513x - 229.5$, and the Landsat 8 OLI image has a regression value of 0.4905 with the equation $y = 707.82x - 84.84$ (see Fig. 2).

The carbon stock information obtained is the carbon value derived from the results of the previous regression equation from the vegetation index input used in each of the three images so that the pixel values in the image are the carbon value information itself. Based on this equation, the vegetation index pixel values that reflect vegetation, especially mangroves, are then added up to obtain biomass information at the research location. Thus, the carbon stock information obtained is a carbon value from pixel values. The number of pixel values that appear at the research location is information that contains carbon values. The resulting maps have different carbon stock levels, so the spatial distribution of carbon stock in each image is also different.

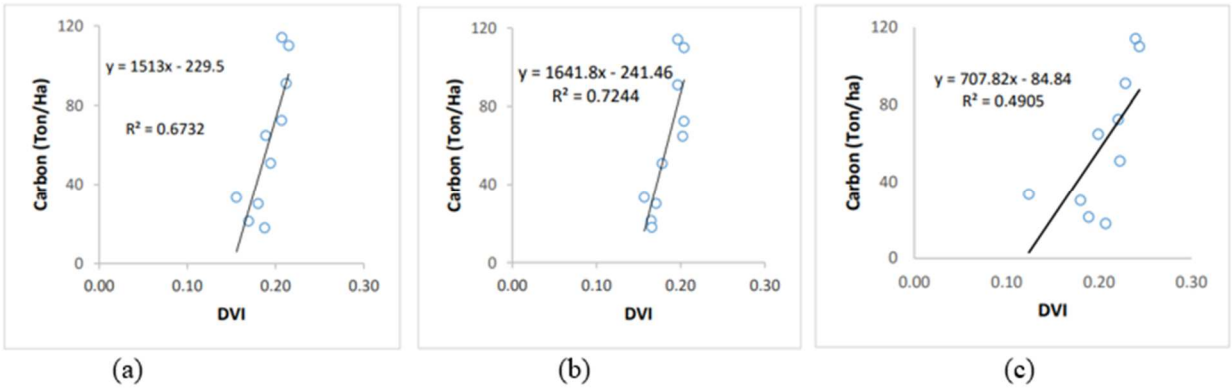

Fig. 2 (a) Planetscope; (b) Sentinel 2A; and (c) Landsat 8 OLI

The spatial distribution resulting from PlanetScope images appears smoother than Sentinel 2A and Landsat 8 OLI images because the spatial resolution of PlanetScope images is relatively high, namely 3 meters (See Fig. 3). Based on the carbon stock map that has been produced, the southern or lower part of the mangrove area has a higher carbon stock and is dominated by blue. This is possible because the vegetation index value of the mangrove area in the southern part is higher than the northern part. Meanwhile, the carbon stock of the south of the mangrove area tends to vary, shown in red, green, and blue, but is dominated by green.

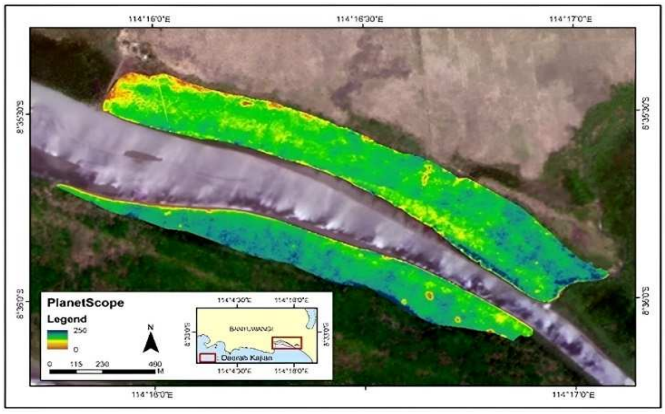

Fig. 3 Spatial distribution of carbon stocks PlanetScope imagery

Like PlanetScope imagery, the spatial distribution map of carbon stocks in Sentinel 2A imagery is obtained from the DVI index. Apart from that, the spatial distribution of carbon stocks in the Sentinel 2A image is not too different from PlanetScope. The southern or lower mangrove area has higher carbon stocks and is dominated by blue. Meanwhile, carbon stocks in the southern mangrove area tend to vary, shown in red, green to blue. Differences in carbon stocks in the southern and northern mangrove areas are possible due to differences in the resulting vegetation index values.

Based on the spatial distribution map created, the Landsat 8 OLI image looks rougher than the other images used. This is because the spatial resolution of the Landsat 8 OLI image is relatively low, namely 30 meters. However, The temporal and spatial amplitude of spectral data from sensors, such as those from the Landsat series, allows the modeling of forest biomass and carbon with a resolution of up to 30 m [25]–[27]. The spatial distribution of carbon stocks produced in the southern and northern mangrove areas is not too different. The map shows that the mangrove areas in the south and north have high carbon stocks, as shown in blue. This is possible because the resulting vegetation index value is higher, which can influence the estimated value of mangrove carbon stocks.

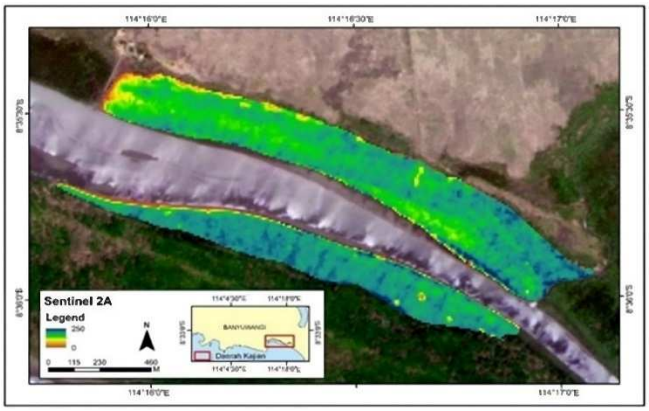

Fig. 4 Spatial distribution of carbon stocks Sentinel 2A imagery

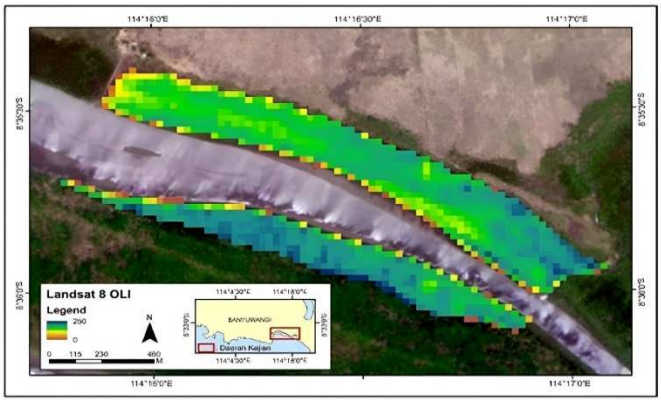

Fig. 5 Spatial distribution of carbon stocks Landsat 8 OLI imagery

The total carbon stock estimation results were obtained from the best regression equation. So, the estimate of total carbon stock results from adding 10 points is used in regression analysis or carbon stock modeling. From these results, the estimate of the total carbon stock for each image is different.

TABLE V
COMPARISON OF TOTAL ESTIMATION RESULTS

No	Planetscope	Sentinel 2A	Landsat 8 OLI
1	66.58	58.67	64.86
2	68.70	60.70	70.88
3	50.57	58.90	50.05
4	57.98	64.83	61.49
5	25.05	48.63	51.55
6	61.26	57.40	61.15
7	48.77	48.31	43.43
8	55.54	50.43	51.20
9	44.01	49.66	22.74
10	56.82	51.70	56.23
	535.27 ton	549.23 ton	533.57 ton

Based on the table above, it can be seen that the estimated total carbon stock value in the Landsat 8 OLI image has the lowest total estimate. In contrast, the Sentinel 2A image has the highest total estimate. This is because the carbon stock value in PlanetScope imagery has a range of between 25 – 68 tons/ha, Sentinel 2A imagery has a range of 48 – 64 tons/ha, and Landsat 8 OLI imagery has a range of between 22 – 70 tons/ha. Even though the maximum value of the carbon stock range in the Landsat 8 OLI image is higher than the other two images, the Sentinel 2A image has a carbon value for each point greater than the other images used in this research. Higher mangrove species diversity in rehabilitated mangroves may support higher productivity and biomass carbon stocks [28], [29].

C. Accuracy

Mapping of mangrove carbon stocks in the Bedul Mangrove Area, Banyuwangi Regency produced three maps from each image used in this research, which are estimates or estimates. This requires an accuracy test to see the accuracy of carbon stock estimates from the three images that depict the carbon stock information produced. accuracy assessment is often discussed because it determines model reliability [30]The accuracy test process uses 10 sample points taken during fieldwork, which are not the sample points used to build the regression equation. The accuracy test results of the input vegetation index in each image produce different SEE values.

TABLE VI
ACCURACY TEST

No	Field Carbon (y)	Planetscope		Sentinel 2A		Landsat 8 OLI	
		Carbon prediction (y‘)	(y-y‘)2	Carbon prediction (y‘)	(y-y‘)2	Carbon prediction (y‘)	(y-y‘)2
1	99.03	43.41	3093.61	26.01	5332.64	21.89	5950.44
2	62.87	64.66	3.19	58.67	17.62	69.30	41.35
3	32.70	56.90	585.35	46.08	546.72	57.25	602.71
4	24.92	57.34	1051.08	60.01	1231.89	52.97	787.29
5	53.66	59.54	34.48	54.47	0.65	62.48	77.73
6	56.98	49.53	55.45	51.50	30.08	48.86	65.98
7	58.00	53.86	17.22	52.81	26.96	45.25	162.78
8	51.27	37.69	184.55	34.57	279.00	36.98	204.45
9	53.56	67.78	202.34	60.38	46.54	70.93	301.89
10	12.86	64.50	2666.58	60.36	2255.77	61.67	2391.32
			31.41		34.94		36.38

Based on the SEE accuracy test results of the three images, the PlanetScope image has the lowest SEE value compared to other images. The SEE value for PlanetScope imagery is 31.41 tones/ha, Sentinel 2A imagery 34.94 tons/ha, and Landsat 8 OLI imagery 36.38 tons/ha. From these results, the PlanetScope image has a lower value than the three images. This reflects that the PlanetScope image has the highest accuracy or has good accuracy compared to other images that have been tested. These findings align with previous studies that reported similar performance of PlanetScope imagery in estimating forest AGB [31] while the Landsat 8 OLI image has the lowest accuracy value because the SEE value of this image is the highest compared to other images. The best AGC empirical model was obtained from PlanetScope and the PlanetScope model contributed the most to improving the accuracy of AGB estimates [32], [33]. The range of predicted carbon values in PlanetScope imagery ranges between 37.69 – 67.78, Sentinel 2A imagery between 26.01 – 60.38, and Landsat 8 OLI imagery between 21.89 – 70.93. In addition to the accuracy test using SE, in this study, the accuracy test used to estimate carbon stocks on the surface of mangroves was carried out using a 1:1 goodness of fit plot. The function of this accuracy method is to try to see whether the estimated data pattern and whether the accuracy test sample has an overestimated or underestimated pattern by looking at the slant of the linear line of the sample plot, which is bounded by the red line as the ideal value of 1:1 between the field value and the estimate. If the distribution of the linear plot is biased toward the image estimation data, then overestimation and underestimation occur when the linear plot is biased toward field data.

Based on the results of accuracy tests using a 1:1 goodness of fit plot for each image, the distribution pattern of mangrove carbon stock estimates shows that the entire model in mapping mangrove carbon stocks is over-estimated. This can be seen from the distribution of points, which tend to be above the line. The overestimated results are possible because more objects around the mangrove, especially canopy density, are recorded by remote sensing sensors compared to tree diameter as input for field carbon results. In the accuracy test results of the 1:1 goodness of fit plot, the R^2 value is very low compared to the R^2 value for the carbon stock model. A low R^2 value indicates that some plots with high vegetation index values do not always have high carbon stocks (See Fig.6).

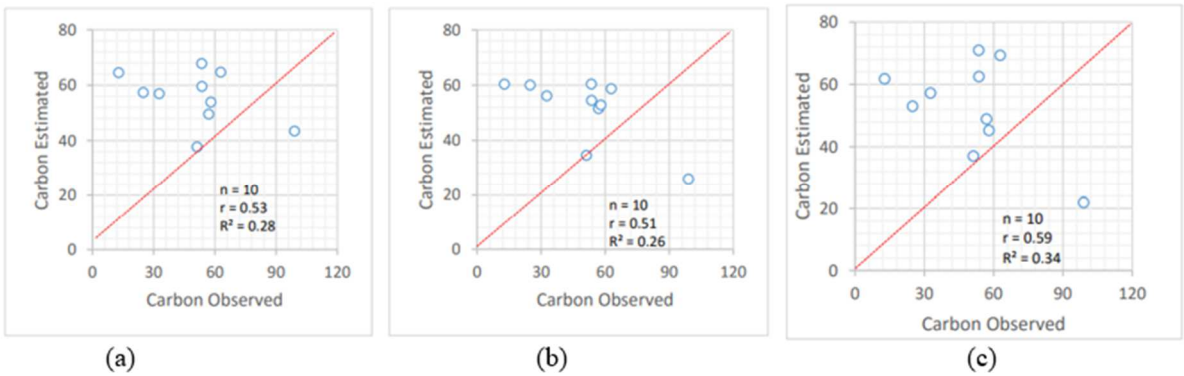

Fig. 6 Plot goodness of fit 1:1 from (a) Planetscope; (b) Sentinel 2A; and (c) Landsat 8 OLI

The composition of mangrove species dramatically influences the relationship between these two parameters. Morphologically, the size of mangroves varies between types, causing carbon stocks to vary. Thus, the dominant mangrove type dramatically determines the size of carbon stocks.

IV. Conclusion

The total carbon obtained from PlanetScope imagery was 535.27 tonnes, Sentinel 2A imagery was 549.23 tonnes, and Landsat 8 OLI imagery was 533.57 tonnes. Among the three images used, based on Sentinel 2A statistical analysis reflects the possibility of overfitting or the best with higher r and R^2 values in the calculations. However, based on SE accuracy tests, PlanetScope has better accuracy than the other two images. Apart from that, the accuracy test results using a 1:1 goodness of fit plot for each image, the distribution pattern of mangrove carbon stock estimates shows that the entire model in mapping mangrove carbon stocks is over-estimated.

Acknowledgment

The authors thank the Alas Purwo National Park management for granting fieldwork permits. We are grateful to R.F. Lestari, S.A. Hafid, S.M. Ridha, A.D. Rahmandhana, M.A. Purnomo, and A. Widodo for their invaluable assistance during the fieldwork.

References

[1] E. D. Candra, Hartono, and P. Wicaksono, "Above Ground Carbon Stock Estimates of Mangrove Forest Using Worldview-2 Imagery in Teluk Benoa, Bali," *IOP Conf. Ser.: Earth Environ. Sci.*, vol. 47, p. 012014, Nov. 2016, doi: 10.1088/1755-1315/47/1/012014.

[2] L. Pendleton *et al.*, "Estimating Global 'Blue Carbon' Emissions from Conversion and Degradation of Vegetated Coastal Ecosystems," *PLoS ONE*, vol. 7, no. 9, p. e43542, Sep. 2012, doi:10.1371/journal.pone.0043542.

[3] B. C. Murray, L. Pendleton, W. A. Jenkins, and S. Sifleet, "*Green Payments for Blue Carbon*".

[4] F. Adelisardou, W. Zhao, R. Chow, P. Mederly, T. Minkina, and J. S. Schou, "Spatiotemporal change detection of carbon storage and sequestration in an arid ecosystem by integrating Google Earth Engine and InVEST (the Jiroft plain, Iran)," *Int. J. Environ. Sci. Technol.*, vol. 19, no. 7, pp. 5929–5944, Jul. 2022, doi:10.1007/s13762-021-03676-6.

[5] J. S. Hall *et al.*, "Deforestation scenarios show the importance of secondary forest for meeting Panama's carbon goals," *Landsc Ecol*, vol. 37, no. 3, pp. 673–694, Mar. 2022, doi: 10.1007/s10980-021-01379-4.

[6] P. Menéndez, I. J. Losada, S. Torres-Ortega, S. Narayan, and M. W. Beck, "The Global Flood Protection Benefits of Mangroves," *Sci Rep*, vol. 10, no. 1, p. 4404, Mar. 2020, doi: 10.1038/s41598-020-61136-6.

[7] T. A. Worthington *et al.*, "Harnessing Big Data to Support the Conservation and Rehabilitation of Mangrove Forests Globally," *One Earth*, vol. 2, no. 5, pp. 429–443, May 2020, doi:10.1016/j.oneear.2020.04.018.

[8] Md. H. Iqbal, "Valuing ecosystem services of Sundarbans Mangrove forest: Approach of choice experiment," *Global Ecology and Conservation*, vol. 24, p. e01273, Dec. 2020, doi:10.1016/j.gecco.2020.e01273.

[9] A. D. Rahmandhana, M. Kamal, and P. Wicaksono, "Spectral Reflectance-Based Mangrove Species Mapping from WorldView-2 Imagery of Karimunjawa and Kemujan Island, Central Java Province, Indonesia," *Remote Sensing*, vol. 14, no. 1, p. 183, Jan. 2022, doi: 10.3390/rs14010183.

[10] V. B. Arifanti, J. B. Kauffman, D. Hadriyanto, D. Murdiyarso, and R. Diana, "Carbon dynamics and land use carbon footprints in mangrove-converted aquaculture: The case of the Mahakam Delta, Indonesia," *Forest Ecology and Management*, vol. 432, pp. 17–29, Jan. 2019, doi: 10.1016/j.foreco.2018.08.047.

[11] M. Basyuni, L. A. P. Putri, and M. B. Murni, "Implication of Land-Use and Land-Cover Change into Carbon Dioxide Emissions in Karang Gading and Langkat Timur Wildlife Reserve, North Sumatra, Indonesia," *Jurnal Manajemen Hutan Tropika (Journal of Tropical Forest Management)*, vol. 21, no. 1, pp. 25–35, Apr. 2015, doi:10.7226/jtfm.21.1.25.

[12] J. Boone Kauffman *et al.*, "The jumbo carbon footprint of a shrimp: carbon losses from mangrove deforestation," *Front Ecol Environ*, vol. 15, no. 4, pp. 183–188, May 2017, doi: 10.1002/fee.1482.

[13] S. D. Sasmito *et al.*, "Mangrove blue carbon stocks and dynamics are controlled by hydrogeomorphic settings and land-use change," *Global Change Biology*, vol. 26, no. 5, pp. 3028–3039, May 2020, doi:10.1111/gcb.15056.

[14] P. Wirabumi, P. Wicaksono, M. Kamal, I. Ridwansyah, L. Subehi, and A. Dianto, "Spatial Distribution Analysis of Total Suspended Solid (TSS) using PlanetScope Data in Menjer Lake, Wonosobo Regency," *JAGI*, vol. 4, no. 1, pp. 289–297, Apr. 2020, doi:10.30871/jagi.v4i1.1853.

[15] P. M. López-Serrano, J. L. Cárdenas Domínguez, J. J. Corral-Rivas, E. Jiménez, C. A. López-Sánchez, and D. J. Vega-Nieva, "Modeling of Aboveground Biomass with Landsat 8 OLI and Machine Learning in Temperate Forests," *Forests*, vol. 11, no. 1, p. 11, Dec. 2019, doi:10.3390/f11010011.

[16] S. Pandit, S. Tsuyuki, and T. Dube, "Estimating Above-Ground Biomass in Sub-Tropical Buffer Zone Community Forests, Nepal, Using Sentinel 2 Data," *Remote Sensing*, vol. 10, no. 4, p. 601, Apr. 2018, doi: 10.3390/rs10040601.

[17] A. Jellouli, A. El Harti, Z. Adiri, E. M. Bachaoui, and A. El Ghmari, "Application of Remote Sensing Data in Lithological Discrimination of Kerdous Inlier in the Anti Atlas Belt of Morocco," *JOIV*, vol. 3, no. 2–2, Aug. 2019, doi: 10.30630/joiv.3.2-2.265.

[18] D. Utari, M. Kamal, and F. Sidik, "Above-ground biomass estimation of mangrove forest using WorldView-2 imagery in Perancak Estuary, Bali," *IOP Conf. Ser.: Earth Environ. Sci.*, vol. 500, no. 1, p. 012011, Jun. 2020, doi: 10.1088/1755-1315/500/1/012011.

[19] E. Purnamasari, M. Kamal, and P. Wicaksono, "Comparison of vegetation indices for estimating above-ground mangrove carbon stocks using PlanetScope image," *Regional Studies in Marine Science*, vol. 44, p. 101730, May 2021, doi:10.1016/j.rsma.2021.101730.

[20] B. S. Nasional, *Pengukuran dan penghitungan cadangan karbon – Pengukuran lapangan untuk penaksiran cadangan karbon hutan (ground based forest carbon accounting)*. BSN, 2011.

[21] A. Komiyama, J. E. Ong, and S. Poungparn, "Allometry, biomass, and productivity of mangrove forests: A review," *Aquatic Botany*, vol. 89, no. 2, pp. 128–137, Aug. 2008, doi:10.1016/j.aquabot.2007.12.006.

[22] M. Kamal, M. F. Hidayatullah, P. Mahyatar, and S. M. Ridha, "Estimation of aboveground mangrove carbon stocks from WorldView-2 imagery based on generic and species-specific allometric equations," *Remote Sensing Applications: Society and Environment*, vol. 26, p. 100748, Apr. 2022, doi:10.1016/j.rsase.2022.100748.

[23] M. Kamal, P. Wicaksono, D. W. Anggara, and M. Hafizt, "Pengaruh Resolusi Spasial Citra Penginderaan Jauh Terhadap Estimasi Leaf Area Index Mangrove di Kepulauan Karimunjawa Jawa Tengah," in *Simposium Nasional Sains Geoinformasi*, Yogyakarta, Indonesia: PUSPICS Fakultas Geografi UGM, Nov. 2015, pp. 667–674.

[24] M. Basyuni *et al.*, "Aboveground biomass and carbon stock estimation using UAV photogrammetry in Indonesian mangroves and other competing land uses," *Ecological Informatics*, vol. 77, p. 102227, Nov. 2023, doi: 10.1016/j.ecoinf.2023.102227.

[25] H. S. J. Zald *et al.*, "Integrating Landsat pixel composites and change metrics with lidar plots to predictively map forest structure and aboveground biomass in Saskatchewan, Canada," *Remote Sensing of Environment*, vol. 176, pp. 188–201, Apr. 2016, doi:10.1016/j.rse.2016.01.015.

[26] J. Zhang, C. Lu, H. Xu, and G. Wang, "Estimating aboveground biomass of Pinus densata-dominated forests using Landsat time series and permanent sample plot data," *J. For. Res.*, vol. 30, no. 5, pp. 1689–1706, Oct. 2019, doi: 10.1007/s11676-018-0713-7.

[27] S. Nunes, L. Oliveira, J. Siqueira, D. C. Morton, and C. M. Souza, "Unmasking secondary vegetation dynamics in the Brazilian Amazon," *Environ. Res. Lett.*, vol. 15, no. 3, p. 034057, Mar. 2020, doi: 10.1088/1748-9326/ab76db.

[28] M. Basyuni, Y. Bimantara, N. T. K. Cuc, T. Balke, and A. G. Vovides, "Macrozoobenthic community assemblage as key indicator for mangrove restoration success in North Sumatra and Aceh, Indonesia," *Restoration Ecology*, vol. 30, no. 7, p. e13614, Sep. 2022, doi: 10.1111/rec.13614.

[29] C. Cameron, L. B. Hutley, D. A. Friess, and B. Brown, "Community Structure Dynamics and Carbon Stock Change of Rehabilitated Mangrove Forests in Sulawesi, Indonesia," *Bulletin Ecologic Soc America*, vol. 100, no. 1, p. e01478, Jan. 2019, doi:10.1002/bes2.1478.

[30] N. H. Quang *et al.*, "Comparisons of regression and machine learning methods for estimating mangrove above-ground biomass using multiple remote sensing data in the red River Estuaries of Vietnam," *Remote Sensing Applications: Society and Environment*, vol. 26, p. 100725, Apr. 2022, doi: 10.1016/j.rsase.2022.100725.

[31] O. Csillik, P. Kumar, and G. P. Asner, "Challenges in Estimating Tropical Forest Canopy Height from Planet Dove Imagery," *Remote Sensing*, vol. 12, no. 7, p. 1160, Apr. 2020, doi: 10.3390/rs12071160.

[32] I. S. Astuty and P. Wicaksono, "Seagrass species composition and above-ground carbon stock mapping in Parang Island using Planetscope image," in *Sixth Geoinformation Science Symposium*, S. B. Wibowo, A. B. Rimba, A. A. Aziz, S. Phinn, J. T. Sri Sumantyo, H. Widyasamratri, and S. Arjasakusuma, Eds., Yogyakarta, Indonesia: SPIE, Nov. 2019, p. 42. doi: 10.1117/12.2549137.

[33] S. D. Madundo, E. W. Mauya, and C. J. Kilawe, "Comparison of multi-source remote sensing data for estimating and mapping above-ground biomass in the West Usambara tropical montane forests," *Scientific African*, vol. 21, p. e01763, Sep. 2023, doi:10.1016/j.sciaf.2023.e01763.